

Optimal kinematic design of a multi-link steering system for a bus independent suspension: An application of response surface methodology

M.M. Topaç*, U. Deryal**, E. Bahar***, G. Yavuz****

*Faculty of Engineering, Dokuz Eylül University, 35397 Izmir, Turkey, E-mail: murat.topac@deu.edu.tr

**Faculty of Engineering, Dokuz Eylül University, 35397 Izmir, Turkey, E-mail: ugur.deryal@ogr.deu.edu.tr

***Faculty of Engineering, Dokuz Eylül University, 35397 Izmir, Turkey, E-mail: egemen.bahar@ogr.deu.edu.tr

****Hexagon Studio, TOSB 1.Cadde 15.Yol No: 7, 41420, Kocaeli, Turkey, E-mail: Guven.Yavuz@hexagonstudio.com.tr

crossref <http://dx.doi.org/10.5755/j01.mech.21.5.11964>

Nomenclature

β_F - steering error; β_L - steering angle of the wheel; β_S - steering wheel angle; β_V - toe angle; CCD - central composite design; DSA - design sensitivity analysis; e_L - unit vector of the steering axis; e_{YR} - unit vector of the wheel rotation axis; FFD - full factorial design; L_F - wheelbase, mm; MSE - maximum steering error, °; O - centre of the bend; S_A - centre of gravity of the vehicle body; s_R - track width, mm; SS - sweep study; Δz_{A_8} - wheel displacement, mm

1. Introduction

Through their design simplicity and ease of manufacturing, Ackerman trapezoidal linkage has a broad application area as the steering system of heavy commercial vehicles equipped with solid axles. On the other hand, as a result of the comfort and control requirements, one of the main targets to be reached in the design of vehicle suspensions is to keep the unsprung mass as small as possible. In order to satisfy these demands, independent front suspensions (IFS) are applied increasingly on busses and trucks by the heavy commercial vehicle manufacturers [1]. In this case, more sophisticated systems are demanded to meet the sufficient steering and independent wheel travel functions simultaneously. Because of its design advantages, multi-link steering linkage (or “opposed four-bar linkage” [2, 3]) is used in the majority of the passenger busses equipped with IFS. This mechanism basically consists of two relay levers, one track rod, two tie rods and two steering arms as seen in Fig. 1.

Kinematic model of a typical bus IFS including

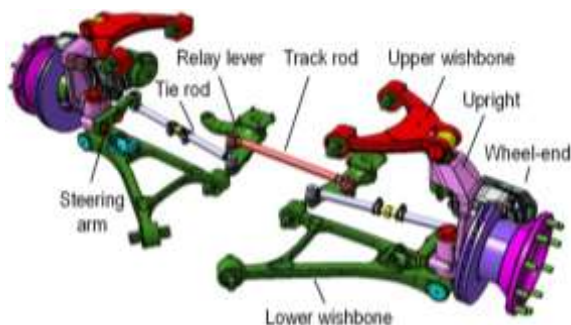


Fig. 1 General view of a bus IFS with the multi-link steering linkage

the multi-link steering linkage is also seen in Fig. 2. Here, A_8 is the centre of mass of the wheel assembly. A_7 is the intersection point of steering axis and wheel rotation axis which are described by the unit vectors e_L and e_{YR} respectively. The co-ordinate system x - y - z is described at the vehicle body centre of gravity S_A . As can be seen from this model, the relay levers are attached to the vehicle body via revolute joints A_{14} . Transmission of the rotational motion between the relay levers is provided by a track rod which is mounted to the relay levers with spherical joints A_{13} . In majority of the busses, assembly of the relay levers and the track rod is planar. Tie rod is also connected to steering arm and relay lever spatially via spherical joints A_9 and A_{10} respectively.

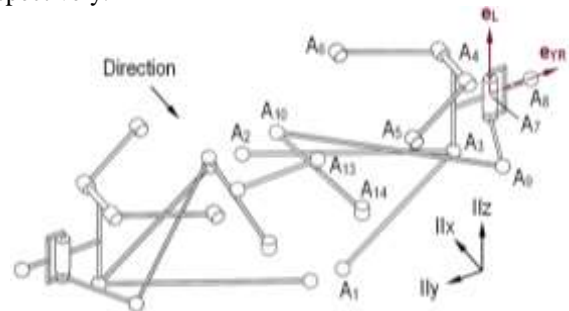


Fig. 2 Kinematic model of the IFS and steering linkage

Generally, one of the main requirements of a vehicle steering mechanism is to give to the steerable wheels a correlated β_L such that, the intersection of the wheel axes should meet at the centre of the bend, O [3, 4]. This rule which can also be seen for a two axle vehicle in Fig. 3 is known as “Ackermann Principle”.

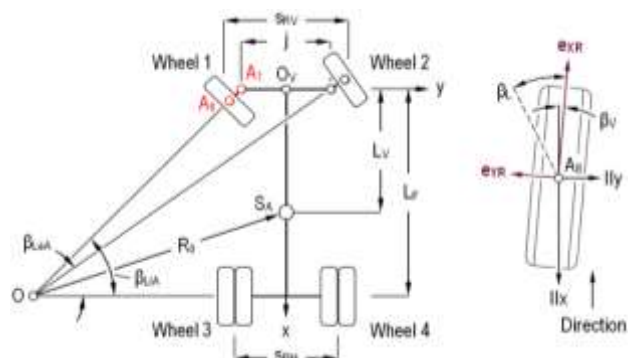


Fig. 3 Ackermann steering geometry and β_V angle of the wheel 1

Mathematically, Ackermann principle can be expressed as:

$$\beta_{LaA}(\beta_{Li}) = \tan^{-1} \frac{1}{\cot \beta_{Li} + \frac{j}{L_F}}, \quad (1)$$

where β_{Li} is the steering angle of the outer wheel and β_{LaA} is the ideal turning angle which is obtained from Eq. (1) for a given steering angle β_{Li} of the inner wheel. The deviation β_F between the ideal steering angle and real turning angle of the wheel which is caused by the steering mechanism geometry is called “the steering error” or “Ackermann error”. Basically, a steering mechanism should satisfy Ackermann principle for given steering error tolerances. β_F can be written as:

$$\beta_F(\beta_{Li}) = \beta_{La}(\beta_{Li}) - \beta_{LaA}(\beta_{Li}). \quad (2)$$

The spatial position of the tie rod of a multi-link steering system also affects the toe (β_V) deviation of the wheel (Fig. 3) as well as MSE. Hence, during the kinematic design process of a multi-link steering mechanism, the deviation of β_V caused by the wheel travel should also be taken into account.

In literature, there are some published works on kinematic optimisation of the steering systems. Zhou et al. optimised a rack-and-pinion steering mechanism by combining MATLAB genetic algorithm toolbox with MSC Adams® to improve steering and β_V characteristics [5]. Hanzaki et al. performed the combined kinematic and sensitivity optimisation of a rack-and-pinion steering linkage used in passenger cars [6]. Oz et al. presented a model validation methodology and the optimisation study on the hardpoints of solid axle suspension and steering systems of a heavy commercial vehicle by using Design of Experiments DOE approach [7]. Liang and Xin optimised the toe deviation of a double wishbone suspension during vertical wheel travel via Adams/View [8]. An interesting paper was published by Kim et al. on the effect of the drag link hardpoints on β_V angle and the deviation of the wheelbase for a solid front axle. In their work, they used a $L_{27}(3^{13})$ type orthogonal array and ANOVA to obtain the optimal combination of design parameters [9]. In open literature, to date and to the best of the authors' knowledge there have been a few works published on the kinematic optimisation the multi-link steering mechanisms for independent suspensions. Bian et al. established the multibody model of the steering mechanism based on the R-W (Robertson and Wittenburg) method for the MacPherson strut [10] and double wishbone suspension [11] for automobiles. In these two works, the suggested models are identical. In summary, all of these works mainly focalise on optimisation of the partial kinematic parameters of a steering system rather than presenting a complete optimization procedure.

In the present study, a response surface-based design procedure to build a multi-link steering system for a passenger bus IFS which satisfies optimum tolerances of β_V and β_F deviations is proposed. A brief summary of the method used in this work is seen in Fig. 4. In stage 1, a multibody model of a bus IFS including the steering mechanism was performed by using MSC Adams® commercial software. In order to compose the IFS model, the hard-

points A_1 to A_8 were drawn from a produced intercity bus. In this model, primary position of the tie rod and the position tolerances of the hardpoints A_9 and A_{10} were chosen by considering the design limitations such as the brake system and the knuckle design. In stage 2, optimal positions of A_9 and A_{10} which directly affect the β_V angle of the front wheels during the wheel travel were determined by using DOE approach via Adams/Insight™ multi-objective optimisation tool. To this end, firstly the most important factors among the Degrees of Freedom (DOF) of A_9 and A_{10} on β_V deviation were chosen via a factorial design-based DSA. Results obtained from FFD study were utilised in MINITAB®, a practical statistical software package [12]. In order to find out the exact optimum locations of A_9 and A_{10} , CCD was also utilised. By using the results, the vertical position of the multi-link mechanism plane was also determined. In stage 3, which is the final phase, MSE was optimised in the β_L range of the front wheels by taking Ackermann principle into account. For this reason, an H-shaped parallel arm mechanism which is the most general from was chosen as the base model for optimisation study. Optimal positions of the hardpoints A_{10} , A_{13} and A_{14} which constitutes the kinematic shape of the relay lever and directly affect the steering error is studied by using a composite method including SS and CCD.

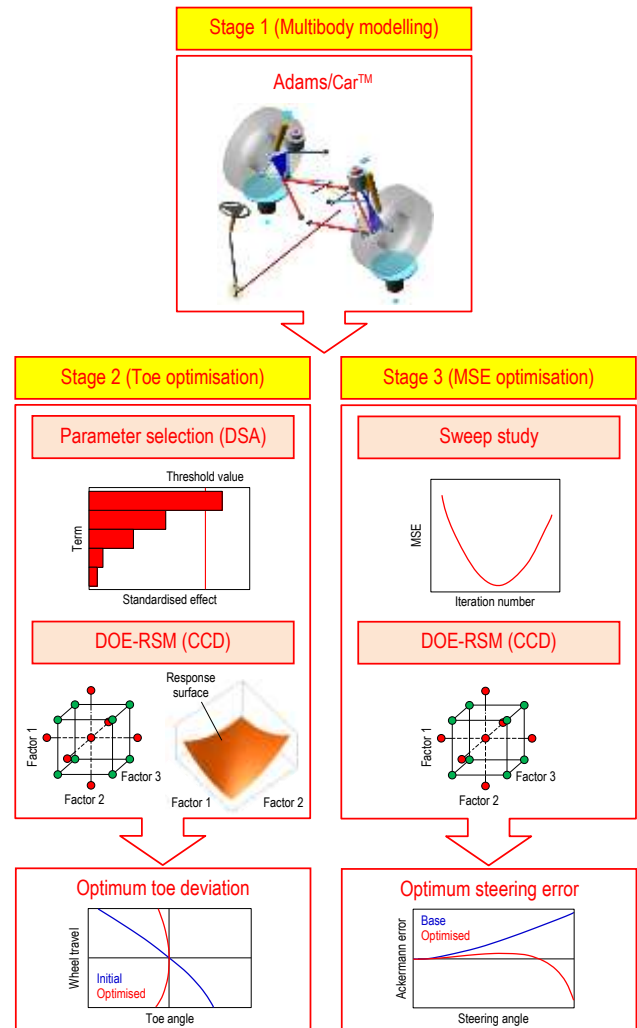


Fig. 4 Summary of the optimisation process

2. Multibody model of the double wishbone suspension

A three dimensional multibody model of the bus IFS including the full steering system is composed by using Adams/Car™ module of MSC. Adams®. In this model which is seen in Fig. 5, Adams/Car™ co-ordinate axis convention was applied [13]. Model consists of 15 elements. Kinematic constraint elements are also shown in Fig. 6. In this model, steering wheel 1 and steering column 2 are directly connected with the upper part of the intermediate shaft 3 via universal joint (U). A translational joint (T) which has single sliding DOF is defined between the upper and lower parts of the intermediate shaft. Lower part is also connected to the rack of the steering box 4 by a universal joint. Pitman arm 5 is fixed to the output shaft and also connected to the drag link 6. The other end of drag link and track rod 8 is mounted to the relay lever 7 via spherical joints (S). In order to reduce the DOF and simplify the model, “Convel” homokinetic joint (C) which has 2 DOF is utilised instead of a 3 DOF spherical joint for relay lever-tie rod 9 connection (A₁₀). Steering arm 10 - tie rod connection is provided by a spherical joint.

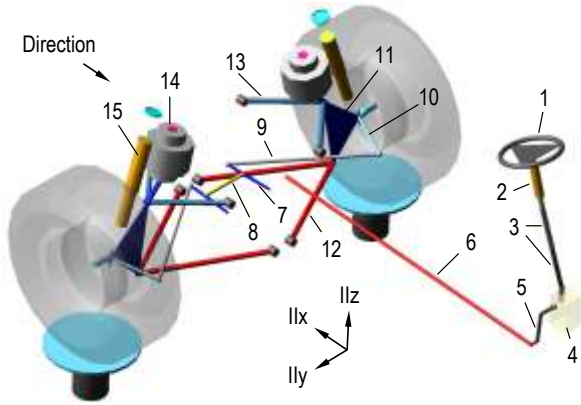


Fig. 5 Multibody model of the bus IFS and steering system

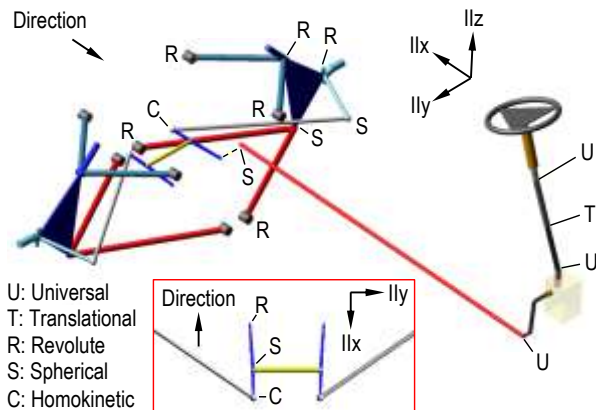


Fig. 6 Kinematic constraints of the steering mechanism

Steering axis is defined as the rotation axis of a revolute joint (R) which is located on the upright 11. Upright is also connected with upper 13 and lower 12 wishbones via revolute and spherical joints. Air spring 15 is directly mounted on upright instead of a wishbone. According to [14, 15] spring rate of the suspension can be assumed as $i_f \approx 1$ (-) for this design type. PAC2002 tyre model [16] was used for tyres with dimensions of 295/80 R 22.5 which is similar those fitted on the bus axles.

3. Methodology

In this study DOE-RSM methods are utilised to determine the optimum values of the parameters providing the desired ranges of β_V deviation and β_r . Optimisation process was carried out by Adams/Insight™ which includes DOE and RSM tools. The DOE approach is used for understanding the correlation between the design parameters of the system and its performance [17]. Essentially, RSM is one of the extended DOE methods which uses a polynomial type regression model $y(x)$ [18]. Principal target of the response surface experiments is to obtain an appropriate model to estimate and analyse the relationship between design variables and system response. For a second order response surface model, the regression model is defined in general form as [19]:

$$y = \beta_0 + \sum_{i=1}^k \beta_i x_i + \sum_{i \leq j}^k \beta_{ij} x_i x_j + \varepsilon. \quad (3)$$

Eq. (3) may also be written in terms of e.g. two variables as:

$$y = \beta_0 + \beta_1 x_1 + \beta_2 x_2 + \beta_3 x_1^2 + \beta_4 x_2^2 + \beta_5 x_1 x_2 + \varepsilon. \quad (4)$$

In order to linearise the regression model, new variables may be expressed as $x_3 = x_1^2$, $x_4 = x_2^2$ and $x_5 = x_1 x_2$. Hence, Eq. (4) can be written as:

$$y = \beta_0 + \beta_1 x_1 + \beta_2 x_2 + \beta_3 x_3 + \beta_4 x_4 + \beta_5 x_5 + \varepsilon. \quad (5)$$

This model can also be expressed in matrix form for M experiments as:

$$y = X\beta + \varepsilon, \quad (6)$$

where

$$y = [y_1, y_2, \dots, y_M]^T; \quad (7)$$

$$X = \begin{bmatrix} 1 & x_{11} & x_{21} & \dots & x_{51} \\ 1 & x_{12} & x_{22} & \dots & x_{52} \\ \dots & \dots & \dots & \dots & \dots \\ 1 & x_{1M} & x_{2M} & \dots & x_{5M} \end{bmatrix}; \quad (8)$$

$$\beta = [\beta_0, \beta_1, \beta_2, \beta_3, \beta_4, \beta_5]^T; \quad (9)$$

$$\varepsilon = [\varepsilon_1, \varepsilon_2, \dots, \varepsilon_M]^T, \quad (10)$$

here y is vector of observations, X is the model matrix, β is the vector which includes the interception parameter β_0 and the partial regression coefficients and ε is the vector of random errors [20], the estimated value of β which minimises ε can be expressed as:

$$\hat{\beta} = (X^T X)^{-1} X^T y. \quad (11)$$

ADAMS/Insight™ uses the method of least squares to estimate the β coefficients in the regression model [21]. In this study, CCD type which is offered in the design specification table of Adams/Insight™ was utilised

for this purpose. The CCD involves the use of a two-level factorial or fraction combined with $2k$ axial or star points. Hence, the design includes factorial points, $2k$ axial points, and total n_c centre runs, yielding a total number of 2^k+2k+n_c runs are carried out to achieve experimental data. A comparison of the two level FFD and the CCD for three factors is seen in Fig. 7.

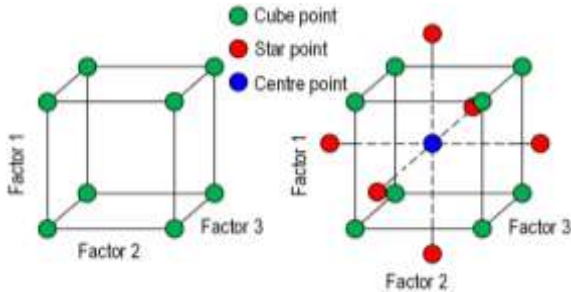


Fig. 7 Comparison of FFD and CCD (according to [17])

Methodology of the study is summarised in Fig. 8.

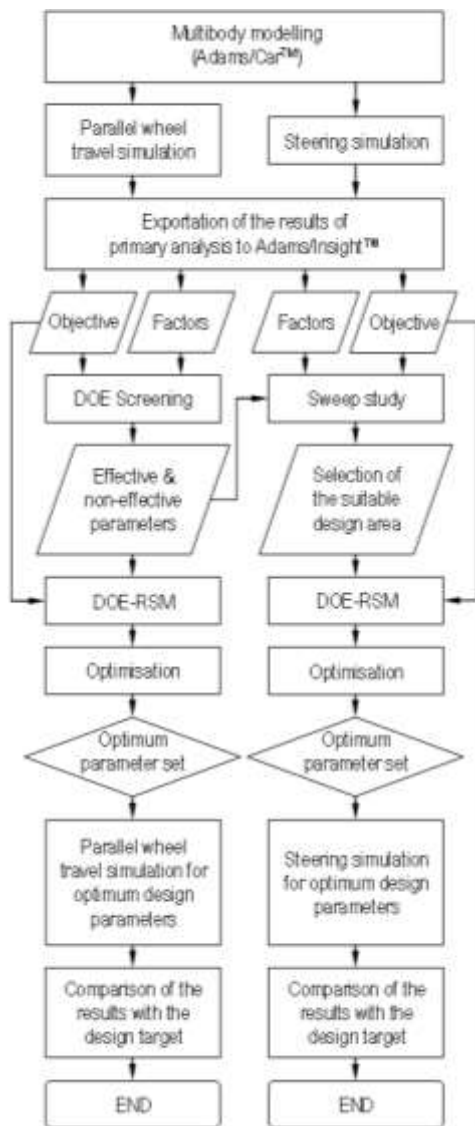


Fig. 8 Flow chart for the optimisation process

At the first stage, a primary simulation (parallel wheel travel or steering) is carried out by using the initial kinematic model generated in Adams/Car™. The design

objective (β_V or β_F) is defined. Except for some differences, optimisation procedures for β_V and β_F are similar. Absolute value of the maximum deviation of the objective obtained from the primary simulation is imported to Adams/Insight™. The factors and design targets are also defined. In the light of the design constraints, the variation ranges of the factors are chosen. Effective and non-effective parameters are identified by screening experiments. Results obtained from these experiments are also used for the SS of β_F optimisation. For the optimisation processes, investigation strategy is chosen as DOE-RSM. Number of the runs is determined according to the design type. The design space and workspace which contain the full set of the design trials and the results of their analyses are generated. Optimum set of the factors which gives the target value of the design objective is obtained by fitting the results to a polynomial or a response surface. In order to control the estimation results of the regression analysis, a multibody model which contains the optimum values of the factors is also carried out. Results obtained from this model are compared with the target value. Some steps of this flow chart have similar characteristics with the methodology given by [22] for the optimisation of the suspension parameters to improve impact harshness (IH) of road vehicles.

4. Toe optimisation

Fig. 9 shows the six total translational DOF of the hardpoints A_9 and A_{10} which determine the position of the tie rod and directly affect the β_V in case of wheel travel. Since tie rod is connected to the relay lever by the spherical joint A_{10} , initial position of the hardpoints A_{13} and A_{14} does not have any remarkable effect on β_V for a given value of β_L . Hence, only the hardpoints of A_9 and A_{10} are chosen as factors in stage 2. A summary of the design limitations are also given in Fig. 10. Here O_V , the midpoint of the front axle was chosen as the reference point for this work. Appropriate positions of the hardpoints A_9 and A_{10} were searched in the design volumes Cube 1 and Cube 2. Initial positions of the cubes and their edge lengths were chosen according to the design limitations which are summarised below. Position of A_9 in x axis should render possible enough space for wheel-end and brake system (Volume B) to eliminate any penetration of the mechanical elements. Initial value of A_{10x} co-ordinate is chosen such that the mechanism should not be blocked in the β_L range of the front wheels. As a design rule, the angles φ and ζ between steering arm and tie rod should not be lower than 15° [2] in

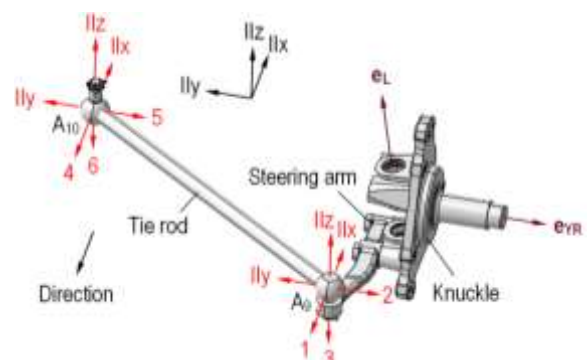


Fig. 9 Factors for A_9 and A_{10}

course of the maximum steering position of the front wheels as seen in Fig. 11.

Steel wheel limits the $-y$ co-ordinate of A_9 because of the installation issues. A gap “ e ” is necessary which limits the $-y$ co-ordinate of A_{10} because of the installation issues. In this design, gap e is assumed as 60 mm by considering the physical diameter of the spherical joint A_{10} .

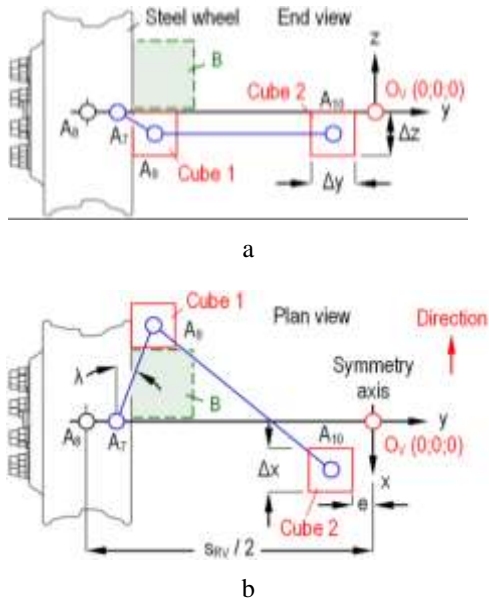


Fig. 10 Summary of design limitations (schematic): a - end view, b - plan view

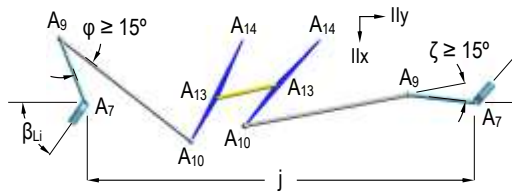


Fig. 11 Full left turn simulation

Because of the design issues, position of the steering arm - knuckle connection is lower than the wheel center A_8 as seen from Fig. 12. Moreover, lower wishbone limits the vertical position of the tie rod. Hence, it is assumed that the vertical (z) co-ordinates of A_9 and A_{10} should be in the range of $z = (0 - 80)$ mm. For this assumption, brake system geometry is also taken into account. Design criterion was chosen such as the β_V should not exceed $\pm 0.3^\circ$ in the wheel travel range of $\Delta z_{A8} = \pm 100$ mm.

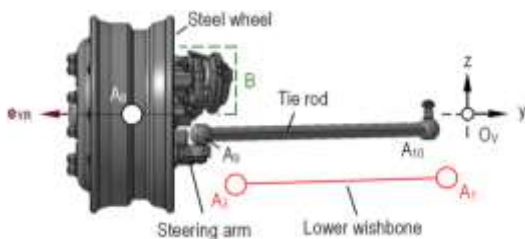


Fig. 12 Design limitations for brake system and wishbone

Before the optimisation process, DSA was applied to determine the effective and non-effective parameters among the tie rod factors on the response of the system. The two-level FFD type was chosen to generate the screen-

ing experiments of the DSA, since it is the most proper type [22]. In this design type, only the lowest and the highest values of each factor are taken into account. As a rule, full factorial design provides 2^n runs for a single screen of experiments where n is the number of the factors. For $n = 6$, FFD provides 64 trials (runs) which is considered as a reasonable experiment number. The results of the trials were fitted to a first order polynomial, whose general form is given in Eq. (5). Schematic of the design model can be seen in Fig. 13. Here, A_9 and A_{10} (the red line) represent the chosen initial position of the tie rod. In Fig. 13, A_{9i} and A_{10i} also stand for the i -th observation as an example (the green line). All of the possible design combinations which connect A_9 and A_{10} were generated by Adams/Insight™ with the use of the cube edges. Successive simulations for every design combination were carried out. Length of the cube edges were chosen as 80 mm.

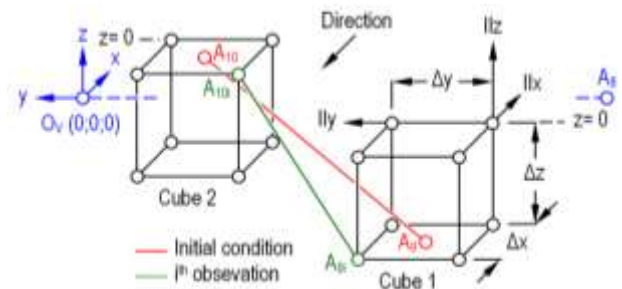


Fig. 13 Model for the tie rod position (schematic)

In order to determine the effects of the factors on β_V clearly, results obtained from the 64 trials given in the design space were imported to MINITAB®, statistical software. Design type was defined as custom factorial design. β_V was also defined as the response of the analysis. The level of significance α was chosen as 0.01. Fig. 14 shows the Pareto chart of the standardised effects obtained from MINITAB® for the total 6 factors of A_9 and A_{10} . In this chart, only the main effects of the DOF's are taken into account. For $\alpha = 0.01$, the threshold value was calculated as $u = 2.665$. Since their standardised effects are greater than this limit, A_{9z} and A_{10z} are predicted as the factors which directly affect the β_V during jounce and rebound. In order to test this result, the co-ordinate A_{9x} which is the most effective factor under the u limit was solely altered in the range of ± 40 mm. It was found that this alteration changed β_V about 2.5% for $z_{A8} = 100$ mm which can be considered as negligible effect.

Since it uses a first order polynomial type regression model, the two level factorial experiments based DSA

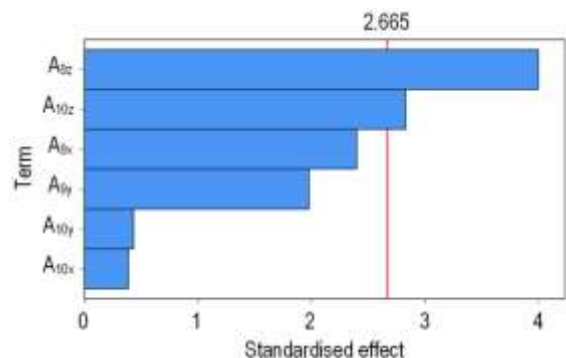


Fig. 14 Pareto chart of the standardised effects ($\alpha = 0.01$)

does not give information about the possible curvature characteristic of the response. Hence, a second order polynomial model whose general form is given in Eq. (3) was utilised. CCD type that is offered in the design specification table of Adams/Insight™ was used to determine the optimum hardpoint locations of the tie rod. Total 50 runs were generated for the CCD process by the software. Optimal hardpoint co-ordinates of the tie rod obtained from Adams/Insight™ are compared with the initial model in Table 1 (for wheel 1). Parallel wheel travel simulation example of the IFS [23] for $\Delta z_{A8} = \pm 100$ mm is seen in Fig. 15.

Table 1
Initial and optimised hardpoint co-ordinates for tie rod

Factor, mm	Initial	Optimised CCD
A9x	-268	-308
A9y	-795	-755
A9z	-80	-55.25
A10x	200	240
A10y	-100	-140
A10z	0	-42.4

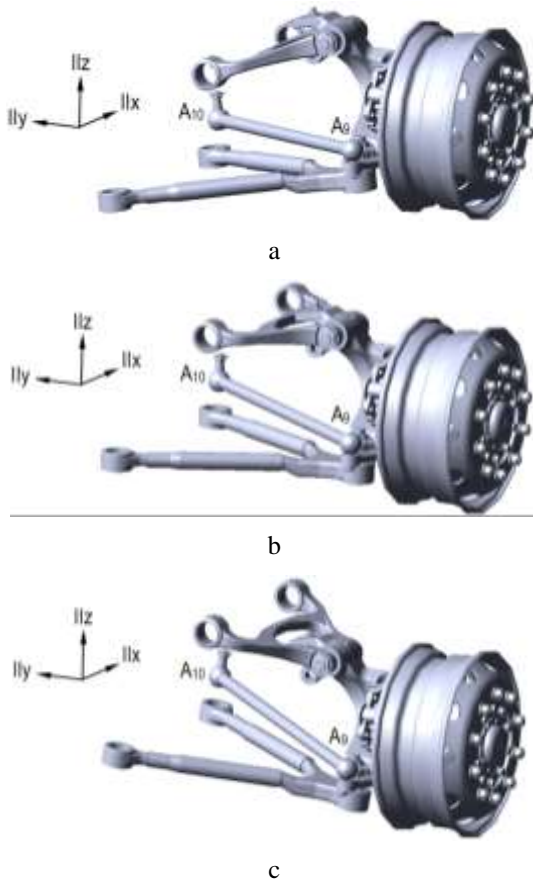


Fig. 15 Parallel wheel travel simulation of the IFS: $\Delta z_{A8} =$:
a - +100 mm; b - 0 mm; c - -100 mm

Deviation characteristics of initial and optimised models are given in Fig. 16. Maximum β_V values were obtained for + 100 mm bump and -100 mm rebound of the wheel as -0.26° and -0.32° respectively.

In order to evaluate the interaction effects of the tie rod factors on β_V deviation, the design matrix obtained from CCD was also imported to MINITAB®. Fig. 17

shows the contour plots obtained from the software for the interactions of the design parameters where, the first term indicates the ordinate and the second is for abscissa.

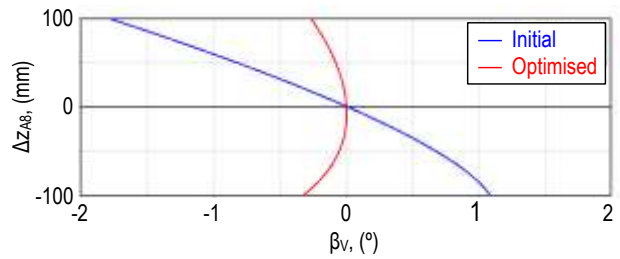


Fig. 16 Comparison of the β_V deviation for initial and optimised designs

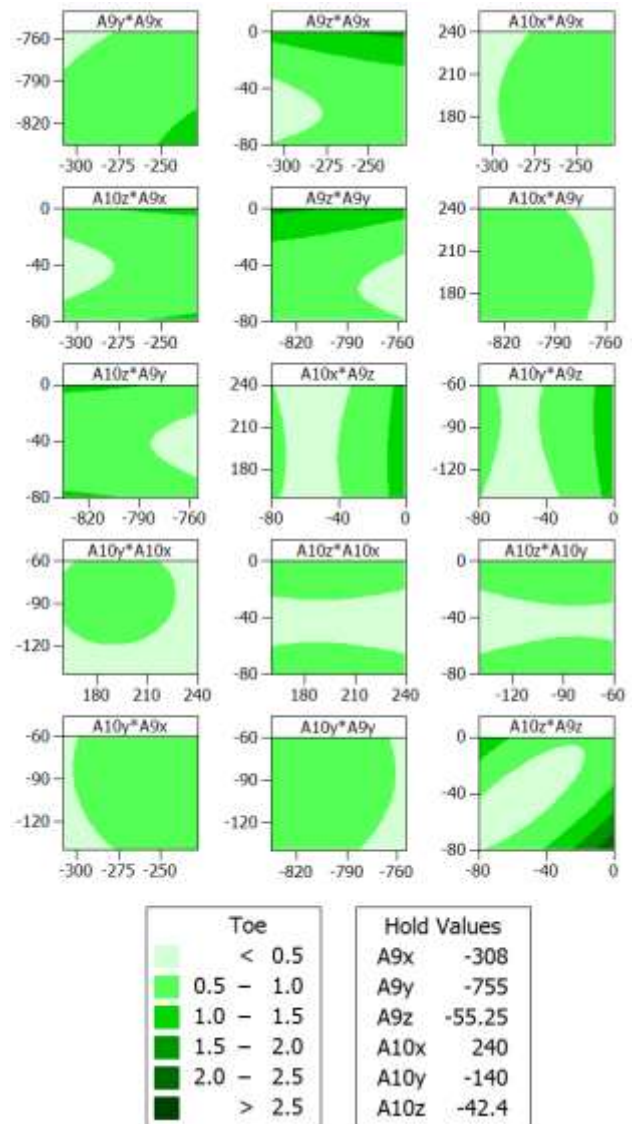


Fig. 17 Contour plots for β_V

In order to obtain these plots, firstly, all of the factors were adjusted to their optimal values (hold values) obtained from CCD (Table 1). Then, only two of the factors were varied in the range of ± 40 mm. As can be clearly seen from the contour plots, β_V deviates strongly along the A_{9z} and A_{10z} axes. The response surface given in Fig. 18 which is identical to contour plot ($A_{10z} * A_{9z}$) also shows that A_{9z} has a greater effect on the β_V than A_{10z} . This result is compatible with the Pareto chart shown in Fig. 14.

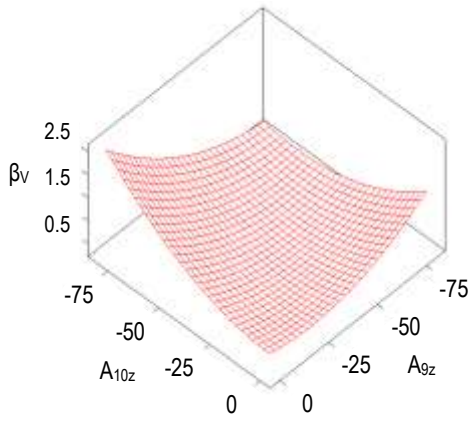


Fig. 18 β_V response as a function of A_{9z} and A_{10z}

5. Steering error optimisation

Basic dimensions of the passenger bus used in this study are seen in Table 2. β_F and MSE values were obtained by taking these values as reference. Since a lower range of β_L is used in most of the driving conditions of a passenger bus, minimising the β_F for this range is acceptable [10, 11].

Table 2

Basic dimensions of the passenger bus (mm)

L_F	L_V	S_{RV}	S_{RH}	j
6050	3957	2096	1825	1844

In this study, design criterion was chosen such as maximum steering error which is defined as:

$$MSE = \max. |\beta_{Li}(\beta_{Li}) - \beta_{LaA}(\beta_{Li})| \quad (12)$$

should not be higher than $\pm 0.5^\circ$ in the range of $\beta_{Li} = \pm 20^\circ$. MSE_{20} is the maximum steering error obtained in $\beta_{Li} = \pm 20^\circ$ range. Fig. 19 shows installation region of the steering system on the bus framework structure (area C) and the base model used in the third stage of this work respectively. In order to optimise MSE , an H-shaped planar parallel arm mechanism which is consisted of two relay levers and a track rod was chosen as the base model.

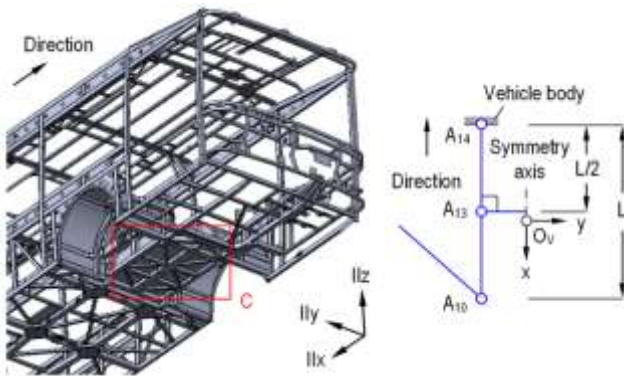


Fig. 19 Bus framework structure and the schematic H-shaped base model for the optimisation study

In this model, initial position of the track rod was selected in the middle of the relay lever. The length L of the relay lever in x axis is directly affects the overall steer-

ing i_S ratio which can be defined as:

$$i_S = \frac{\beta_S}{\beta_L}, \quad (13)$$

where, β_S is the steering wheel angle. In this study, possible range of i_S was chosen in the range of 18-23 (-) due to the manufacturers demand. Effect of relay lever length on i_S of the base mechanism can be seen as a function of β_S in Fig. 20. L_1 was chosen as 540 mm.

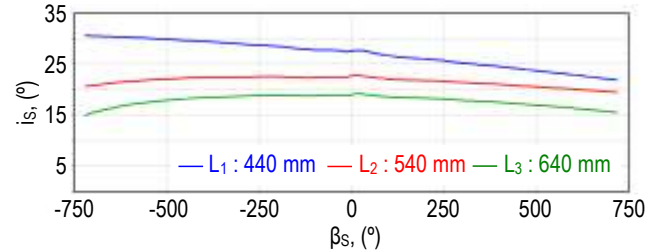


Fig. 20 Effect of the relay lever length on i_S

Design schematic of the relay lever-vehicle body connection is illustrated upside down in Fig. 21. Here, the longitudinal rails M are welded to the lateral rail N on which the bearing of A_{14} is located. In order to find out the appropriate design range for optimisation of the relay lever, a pre-study includes the SS option of Adams/Insight™ was carried out. In this type of design study, the possible range of a factor is determined by taking the design limitations into account. The chosen number of runs specifies how the factor interval will be divided [21]. Results of the runs give an estimation for the deviation characteristic of the MSE_{20} response.

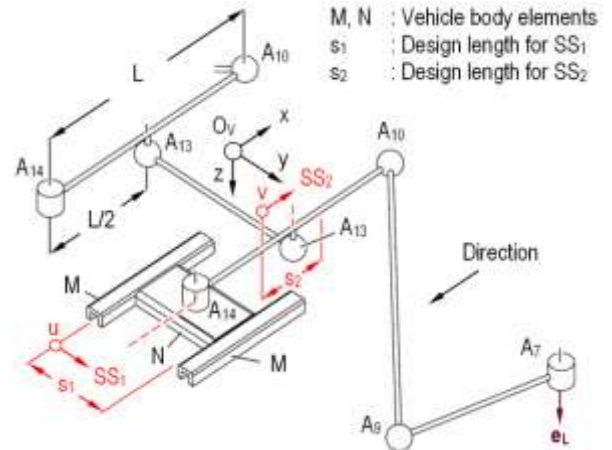


Fig. 21 Design detail of the vehicle body-relay lever connection

In this work, SS is performed in two successive steps: Primary position of A_{10} was assumed as fixed in x - y plane. Position of hardpoint A_{14} was changed in y axis in the range of ± 50 mm. Dimensions of the rails on which relay lever attached via A_{14} bearings were taken into account to determine this design limit. In Fig. 21, u represents the initial trial point of the SS_1 . Step size was chosen as 5 mm for the total $s_1 = 100$ mm design length. 21 trials were generated. As can be seen from the convergence history of SS_1 shown in Fig. 22, minimum value of MSE_{20} was obtained at trial 19 as $MSE_{20} = 0.525^\circ$. Here, trial 11 represents the base model. In the subsequent step, hard-

point A_{14} was adjusted to the minimum value obtained from SS_1 . Then, the planar position of track rod was altered only in x axis in the range of ± 50 mm. Step size was also chosen as 5 mm for the total $s_2 = 100$ mm design length. For SS_2 , 21 trials were generated where v represents the initial trial point. Convergence history of the SS_2 shows that (Fig. 22) trial 10 provides an estimated optimum value of MSE_{20} which is calculated as 0.524° . All of the trials of SS_1 and SS_2 were analysed for $\beta_s = +420^\circ$ which corresponds to $i_s \approx 21$ and $\beta_{Li} \approx 20^\circ$.

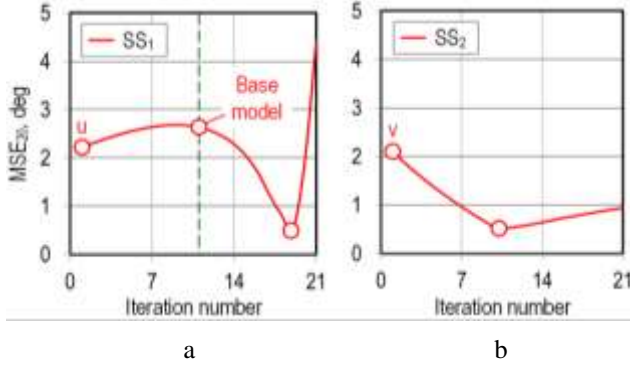


Fig. 22 Convergence histories for: a - SS_1 ; b - SS_2

Since the main target of the SS_1 and SS_2 is to predict the reasonable design range of the hardpoints for the multi-link mechanism, results obtained from these studies are rough. These results were used to perform a final optimisation process using CCD. According to research [23], λ angle (Fig. 11) also affects the steering error. Because of this, A_{9x} and A_{9y} should also be taken into account for the CCD study. Hence, A_9 , A_{10} , A_{13} and A_{14} were chosen as the design variables. On the other hand, in order not to increase the β_V deviation during the wheel travel, all of the factors cannot be used for the optimisation process. As can be seen from the Pareto chart in Fig. 14, A_{10x} and A_{10y} which have lower standardised effects than $u = 2.665$ can be chosen as design variables for the relay lever. Because of the planarity of the mechanism, A_{13z} and A_{14z} were assumed as equal to A_{10z} obtained from CCD. Variation range of the factors was chosen in x - y plane as ± 10 mm except A_{9x} and A_{13x} . In order to shorten the design length of the steering arm, design constraint for A_{9x} was selected as (0-40) mm. It is known from Pareto chart that this alteration does not have any remarkable effect on the β_V angle. A_{13x} range was also selected as (0-30) mm to increase the rigidity of the frame. By using CCD option of Adams/Insight™ 88 trials were generated by the software for 8 factors. Convergence history can be seen in Fig. 23 where minimum MSE_{20} was obtained as $\approx 0.2^\circ$. By using the optimal hardpoint co-ordinates obtained from Adams/Insight™ which are compared with the base model in Table 3, a final multibody model was composed and analysed via Adams/Car™.

Comparison of the base and optimal multi-link model geometries is seen in Fig. 24. It was found that, for the optimised model, ζ angle between tie rod and steering arm satisfies $\zeta \geq 15^\circ$ condition. ζ was obtained as $\zeta \approx 20^\circ$ for $\beta_{Li} = 55^\circ$ which portrays the extreme steering condition. For the optimal design, the angle between the line $|A_{10}-A_{14}|$ and the x axis was calculated as $\zeta_{opt} \approx 4.5^\circ$. MSE_{20} was achieved as 0.34° .

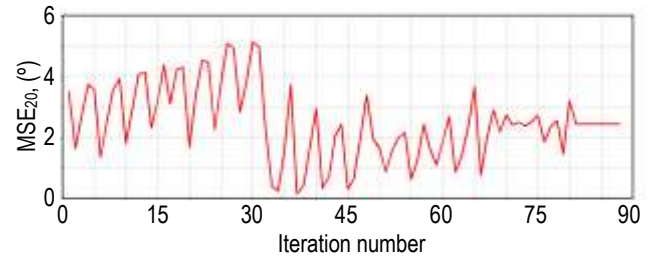


Fig. 23 Convergence history of CCD (estimations)

Table 3
Hardpoint co-ordinates of base and optimised models

Factor (mm)	Base	Optimised CCD
A9x	-308	-270.7
A9y	-755	-746.49
A10x	240	-240.83
A10y	-140	-140.3
A13x	-28.5	-1.9
A13y	-140	-140.41
A14x	-300	-296.32
A14y	-140	-182.77

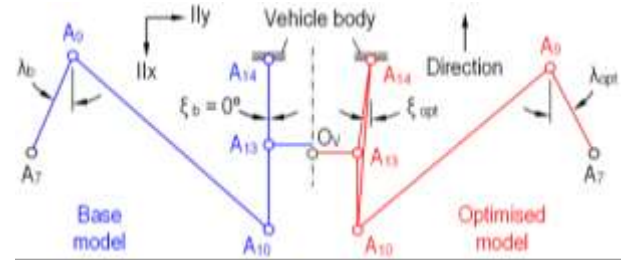


Fig. 24 Comparison of the base and optimised geometries

Obtained minimum values and percent reductions of MSE_{20} after every step of the optimisation study are given in Table 4 and in Fig. 25 respectively. In Fig. 25, a, the estimated MSE_{20} values for SS_1 , SS_2 and CCD are compared with β_F (β_{Li}) = 2.22° that is also obtained from the base model for $\beta_{Li} = 20^\circ$.

Table 4
Estimated and obtained MSE_{20} values ($\beta_{Li} \approx 20^\circ$)

Estimations			Final model	Design target
SS_1	SS_2	CCD	0.34°	$\leq \pm 0.5^\circ$
0.525°	0.524°	0.2°		

In order to calculate the percent reduction, MSE_{20} of the base model was assumed as 100%. As can be seen from Fig. 25, a, MSE_{20} dramatically decreases after SS_1 where the reduction was calculated as 80.1% in comparison with the base model. MSE reduction after SS_2 and CCD were also calculated as 0.04% and 12.3% respectively. Hence, it can be concluded that the most effective factor on MSE_{20} reduction is A_{14y} or the ζ angle. Additionally, it should be noted that the calculated MSE_{20} obtained from SS_1 , SS_2 and CCD are the estimated values. MSE_{20} provided from the multibody analyses of base and final optimised models are also given in Fig. 25, b. Total reduction of MSE_{20} was obtained as 84.8%.

Ackermann error deviations of the base and the optimised models as a function of β_{Li} are given in Fig. 26. As also can be seen that MSE achieved from the final op-

timised model is 0.46° at $\beta_{Li} = 30^\circ$ in the range of $\beta_{Li} = (0-44^\circ)$ which exceedingly satisfies the design target. For instance, by using Eq. (1) β_{Li} is calculated as 33.14° for $R_{0min} = 10.4$ m, the minimum turning radius of the passenger bus and the dimensions given in Table 2. Steering error of the base mechanism was obtained for $\beta_{Li} = 30^\circ$ as 4.4° which means the reduction by 89.6%.

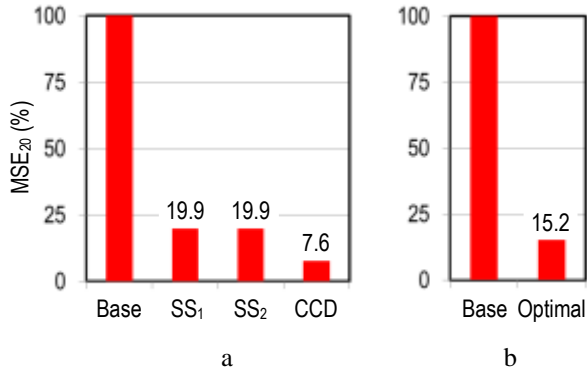


Fig. 25 Reduction of MSE_{20} : a - estimations during the optimisation stages; b - comparison of base and optimised models

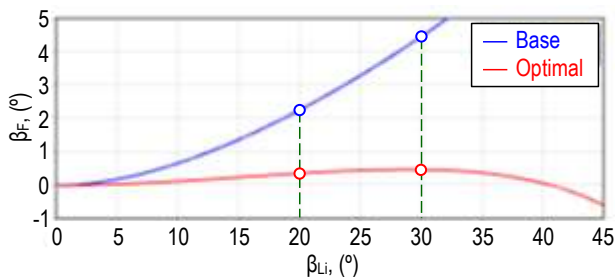


Fig. 26 Comparison of the β_F (β_{Li}) curves for base and optimised models

6. Conclusions

In this work, a DOE-RSM based design application to obtain a multi-link steering mechanism which gives optimum deviation of β_V and steering error was developed and applied on an MSC.Adams[®] multibody model of a bus IFS. In order to carry out the optimisation of the β_V , the most effective parameters among the tie rod co-ordinates on β_V deviation were first identified via DSA by using Adams/Insight[™] multi-objective optimisation tool. The FFD was used to determine the rank of importance of the co-ordinates of the tie rod hardpoints on β_V angle. Results were evaluated by using MINITAB[®] a practical statistical software package. Since the FFD merely uses the high and low values of the factors, it is not adequate to determine the possible curvature of the response. In order to find out the intermediate values of the parameters which give the optimal tie rod position, CCD was also applied. In the final stage of the study, geometry of the steering trapezoid which gives the optimum MSE was determined via SS and CCD. In order to do that the co-ordinate A_{10z} was assumed as the design constraint which determines the vertical position of the multi-link mechanism plane. Results obtained from this study are summarised as follows:

1. Results of the DSA showed that for a multi-link steering mechanism, the most effective factors among the tie rod co-ordinates on β_V are the vertical components A_{9z}

and A_{10z} . For this design example, percent effects of A_{9z} and A_{10z} were calculated as 44.71% and 31.76% respectively. CCD gives the optimum values of these co-ordinates more precisely than the FFD with a fewer number of design trials.

2. By using CCD, β_V deviation during the wheel travel was reduced up to 85.4% in comparison with the initial design. Maximum β_V values were obtained for +100 mm bump and -100 mm rebound of the wheel as -0.26° and -0.32° respectively.

3. By optimizing the shape of the relay lever, MSE of the initial parallel arm (H-shaped) base mechanism was reduced up to 89.6% via SS_1 , SS_2 and CCD in the range of $\beta_{Li} = \pm 44^\circ$. It is observed that the most effective part of the estimation analyses on MSE reduction is SS_1 . By this way it can be concluded that co-ordinate A_{14y} (or the angle ζ) has the greatest effect on MSE . In this design, effect of SS_2 can be assumed as negligible.

4. The obtained optimal mechanism satisfies the design target of $MSE \leq \pm 0.5^\circ$ in the range of $\beta_{Li} = \pm 44^\circ$. Moreover, the mechanism can perform its function up to $\beta_{Li} = 55^\circ$ without any lock up effect.

Acknowledgements

The authors are grateful for the suggestions of Prof. N. S. Kuralay, Ph.D. of Dokuz Eylül University, Department of Mechanical Engineering. The licensed software support of Hexagon Studio is also acknowledged.

References

1. **Timoney, E.; Timoney S.** 2003. A review of the development of independent suspension for heavy vehicles, 2003 SAE International Truck and Bus Meeting and Exhibition, SAE Technical Paper 2003-01-3433. <http://dx.doi.org/10.4271/2003-01-3433>.
2. **Reimpell, J.** 1974. Fahrwerktechnik, Bd. 3, Würzburg: Vogel-Verlag, 177p.
3. **Reimpell, J.; Stoll, H.; Betzler, J.W.** 2002. The Automotive Chassis: Engineering Principles, Warrendale, PA.: Society of Automotive Engineers, Inc.
4. **Simionescu, P.A.; Beale, D.** 2002. Optimum synthesis of the four-bar function generator in its symmetric embodiment: the Ackermann steering linkage, Mechanism and Machine Theory 37(12): 1487-1504. [http://dx.doi.org/10.1016/S0094-114X\(02\)00071-X](http://dx.doi.org/10.1016/S0094-114X(02)00071-X).
5. **Zhou, B.; Li, D.; Yang, F.** 2009. Optimization design of steering linkage in independent suspension based on genetic algorithm, IEEE 10th International Conference on Computer-Aided Industrial Design & Conceptual Design: CAID&CD. Wenzhou, 45-48p. <http://dx.doi.org/10.1109/CAIDCD.2009.5374895>.
6. **Hanzaki, A.R.; Rao, P.V.M.; Saha, S.K.** 2009. Kinematic and sensitivity analysis and optimization of planar rack-and-pinion steering linkages, Mechanism and Machine Theory 44(1) 42-56. <http://dx.doi.org/10.1016/j.mechmachtheory.2008.02.014>.
7. **Oz, Y.; Ozan, B.; Uyanik, E.** 2012. Steering system optimization of a Ford heavy-commercial vehicle using kinematic & compliance analysis, SAE Technical Paper 2012-01-1937. <http://dx.doi.org/10.4271/2012-01-1937>.

8. **Liang J.; Xin, L.** 2012. Simulation analysis and optimization design of front suspension based on ADAMS, *Mechanika* 18(3): 337-340.
<http://dx.doi.org/10.5755/j01.mech.18.3.1873>.
9. **Kim, B.; M., Kim, J.W.; Moon, I.D.; Oh, C.Y.** 2014. Optimal combination of design parameters for improving the kinematics characteristics of a midsize truck through design of experiment, *Journal of Mechanical Science and Technology* 28(3): 963-969.
<http://dx.doi.org/10.1007/s12206-013-1167-7>.
10. **Bian, X.L.; Song, B.A.; Becker, W.** 2003. The optimization design of the McPherson strut and steering mechanism for automobiles, *Forschung im Ingenieurwesen* 68(1): 60-65.
<http://dx.doi.org/10.1007/s10010-003-0107-6>.
11. **Bian, X.L.; Song, B.A.; Walter, R.** 2004. Optimization of steering linkage and double wishbone suspension via R-W multibody dynamic analysis, *Forschung im Ingenieurwesen* 69(1): 38-43.
<http://dx.doi.org/10.1007/s10010-004-0136-9>.
12. Minitab User's Guide 1: Data Graphics and Macros (Release 13 for Windows), 1999. Pennsylvania State University, USA.
13. MSC.Adams®. 2002. Product Catalog. MSC. Software Corporation.
14. **Blundell, M.; Harty, D.** 2006. *The Multibody Systems Approach to Vehicle Dynamics*, London: Elsevier Butterworth – Heinemann, 172p.
15. **Matschinsky, W.** 2007. *Radführungen der Straßenfahrzeuge*. 3. aktualisierte und erweiterte Auflage, Berlin Heidelberg: Springer-Verlag, 96, 97p.
16. **Kuiper, E.; Van Ooster, J.J.M.** 2007. The PAC2002 advanced handling tire model, *Vehicle System Dynamics: International Journal of Vehicle Mechanics and Mobility*, 45(1): 153-167.
<http://dx.doi.org/10.1080/00423110701773893>.
17. **Montgomery, D.C.** 2000. *Design and analysis of experiments*. Fifth Edition, Hoboken, New Jersey: John Wiley & Sons, Inc. 275p.
18. **Park, K.; Heo, S.J.; Kang, D.O.; Jeong, J.I.; Yi, J.H.; Lee, J.H.; Kim, K.W.** 2013. Robust design optimization of suspension system considering steering pull reduction, *International Journal of Automotive Technology* 14(6): 927-933.
<http://dx.doi.org/10.1007/s12239-013-0102-3>.
19. **Han, H.; Park, T.** 2004. Robust optimal design of multi-body systems, *Multibody system dynamics* 11(2): 167-183.
<http://dx.doi.org/10.1023/B:MUBO.0000025414.28789.34>.
20. **Myers, R.H.; Montgomery, D.C.; Anderson-Cook, C.M.** 2009. *Response Surface Methodology: Process and Product Optimization Using Design of Experiments*, Third Edition. Hoboken, New Jersey: John Wiley & Sons, Inc. 704 p.
21. MSC.ADAMS®. 2013. *ADAMS/Insight™ User Guide*. MSC. Software Corporation.
22. **Aydın, M.; Ünlüsoy, S.** 2012. Optimization of suspension parameters to improve impact harshness of road vehicles, *The International Journal of Advanced Manufacturing Technology* 60(5-8): 743-754.
<http://dx.doi.org/10.1007/s00170-011-3589-7>.
23. **Genta, G.** 1997. *Motor Vehicle Dynamics*, Singapore: World Scientific Publishing Co. Pte. Ltd., Regal Pres (S) Pte. Ltd. 216p.

M. M. Topaç, U. Deryal, E. Bahar, G. Yavuz

OPTIMAL KINEMATIC DESIGN OF A MULTI-LINK STEERING SYSTEM FOR A BUS INDEPENDENT SUSPENSION: AN APPLICATION OF RESPONSE SURFACE METHODOLOGY

S u m m a r y

A response surface-based design application to obtain an optimum multi-link steering mechanism is presented. Design problem is essentially established on two main goals: minimum deviation of toe angle (β_V) during the wheel travel and optimum steering error during the steering angle (β_L) range of the wheel. In the first stage, a complete multibody model of the suspension system including the steering mechanism was composed by using MSC.Adams® software. In order to identify the most effective parameters among the tie rod co-ordinates on β_V deviation, a Full Factorial Design (FFD) - based Design Sensitivity Analysis (DSA) was carried out via Adams/Insight™ multi-objective optimisation tool. Central Composite Design (CCD) was also implemented to find out the optimum position of the tie rod. In the final stage, optimum hard-point positions of the steering mechanism were searched by a combination of sweep study (SS) and CCD to provide the minimum deviation of Ackermann error. The optimisation results show that it is possible to reduce the maximum steering error (MSE) of the system up to 89.6 % in comparison with the parallel arm base mechanism by using the proposed methodology.

Keywords: Ackermann steering, central composite design (CCD), design of experiments (DOE), independent front suspension (IFS), maximum steering error (MSE), multi-link steering system, optimisation, regression, response surface methodology (RSM).

Received April 17, 2015

Accepted June 23, 2015